Effects of δ mesons in relativistic mean field theory

Shailesh K. Singh, S. K. Biswal, M. Bhuyan, and S. K. Patra
Institute of Physics, Bhubaneswar - 751005, India

(Received 18 September 2013; revised manuscript received 10 February 2014; published 3 April 2014)

The effect of δ- and ω-ρ-meson cross couplings on asymmetry nuclear systems are analyzed in the framework of an effective field theory motivated relativistic mean field formalism. The calculations are done on top of the G2 parameter set, where these contributions are absent. To show the effect of δ meson on the nuclear system, we split the isospin coupling into two parts: (i) g_ρ due to ρ meson and (ii) g_δ for δ meson. Thus, our investigation is based on varying the coupling strengths of the δ and ρ mesons to reproduce the binding energies of the nuclei ^{48}Ca and ^{208}Pb. We calculate the root mean square radius, binding energy, single particle energy, density, and spin-orbit interaction potential for some selected nuclei and evaluate the L_{sym} and E_{sym} coefficients for nuclear matter as function of δ- and ω-ρ-meson coupling strengths. As expected, the influence of these effects are negligible for the symmetric nuclear system, but substantial for the contribution with large isospin asymmetry.

DOI: 10.1103/PhysRevC.89.044001 PACS number(s): 21.65.Cd, 21.10.Dr, 21.30.Fe, 26.60.Kp

I. INTRODUCTION

In recent years the effective field theory approach to quantum hadrodynamic (QHD) has been studied extensively. The parameter set G2 [1,2], obtained from the effective field theory motivated Lagrangian (E-RMF) approach, is very successful in reproducing the nuclear matter properties including the structure of neutron star as well as of finite nuclei [3]. This model reproduces well the experimental values of binding energy, root mean square (rms) radii, and other finite nuclear properties [4–6]. Similarly, the prediction of nuclear matter properties including the phase transition as well as the properties of a compact star are remarkably good [3,7]. The G2 force parameter is the largest force set available, in the relativistic mean field model. It contains almost all interaction terms of the nucleon with mesons, self-, and cross coupling of mesons up to fourth order.

In the effective-field-theory–motivated relativistic mean field (E-RMF) model of Furnstahl *et al.* [1,2], the coupling of the δ meson is not taken into account. Also, the effect of ρ- and ω-meson cross coupling was neglected. It is soon realized that the importance of the δ meson [8] and the cross coupling of ω and ρ mesons [9] cannot be neglected while studying the nuclear and neutron matter properties. Horowitz and Piekarewicz [10] studied explicitly the importance of ρ and ω cross coupling to finite nuclei as well as the properties of neutron star structures. This coupling also influences the nuclear matter properties, such as symmetry energy E_{sym}, slope parameters L_{sym}, and curvature K_{sym} of E_{sym} [11]. It is shown in Ref. [3] that the self- and cross couplings of the ω meson play an important role to make the nuclear equation of state (EOS) softer [12–14]. The observation of Brown [15], and later on by Horowitz and Piekarewicz [10], makes it clear that the neutron radius of heavy nuclei has a direct correlation with the EOS of compact star matter. It is shown that the collection of neutron to proton radius difference $\triangle r = r_n - r_p$ using relativistic and nonrelativistic formalisms shows two different patterns. Unfortunately, the error bar in the neutron radius makes no difference between these two patterns. Therefore, the experimental result of JLab [16] is greatly anticipated. To have a better argument for all this, Horowitz and Piekarewicz [10] introduced Λ_s and Λ_v couplings to take care of the skin thickness in ^{208}Pb as well as the crust of a neutron star. The symmetry energy, and hence the neutron radius, plays an important role in the construction of asymmetric nuclear EOS. Although, the new couplings Λ_s and Λ_v take care of the neutron radius problem, the effective mass splitting between neutron and proton is not taken care of. This effect cannot be neglected in a highly neutron-rich dense matter system and drip-line nuclei. In addition to this mass splitting, the rms charge radius anomaly of ^{40}Ca and ^{48}Ca may be resolved by this scalar-isovector δ-meson inclusion to the E-RMF model.

In some of the calculations, although the scalar field in the isovector channel is not included explicitly, the Fock term in the currently used relativistic Hartree-Fock and Hartree-Fock-Bogoliubov calculations contains contributions to the scalar-isovector channel [17–20]. It is known that the covariant density functional theory is unable to produce Gamow-Teller resonance (GTR) and spin-dipole resonance (STR) properly, where the Fock term is not present. So there needs to be some further extension in the model, but after zero-range reduction and the Fierz transformation, one can get the GTR and STR without taking the Fock term into account. It shows that zero-range reduction and Fierz transformation are the alternative to the inclusion of the Fock term and avoid a complicated numerical procedure. It gives better results for the spin-isospin channel and Dirac masses [21]. Other contributions in the isoscalar channel are based on the Hugenholtz–Van Hove theorem [22]. According to this theorem, nuclear symmetry energy and the neutron-proton effective k-mass splitting are explicitly related [23]. Our aim in this paper is to include the scalar-isovector δ meson to the interaction and to see its effect along with the ρ-ω-meson couplings in a highly asymmetric system, such as asymmetry finite nuclei, neutron star, and asymmetric EOS.

The paper is organized as follows. First of all we extended the E-RMF Lagrangian by including the δ meson and the ω-ρ cross couplings. The field equations are derived from the extended Lagrangian for finite nuclei. Then the equations of state for nuclear matter and neutron star matter are derived.

The calculated results are discussed in Sec. III. In this section, we study the effects of the δ meson and ω-ρ cross coupling on finite nuclei and see the changes in binding energy, radius, etc. Then, we adopt the calculations for asymmetric nuclear matter, including the neutron star. In the last section, the conclusions are drawn.

II. FORMALISM

The bulk properties, such as binding energy and charge radius, do not isolate the contribution from the isoscalar or isovector channels. These are estimated by an overall fitting of the parameters, precisely with the help of the ρ-meson coupling. That is the reason the modern relativistic Lagrangian ignores the contribution of the δ and ρ mesons separately, i.e., once the ρ meson is included, it takes care of the bulk properties of the nucleus arising from the isovector part and does not feel the requirement of the δ meson [17–20]. However, the importance of the δ meson is realized when we study the properties of the highly asymmetric system, such as drip-line nuclei and neutron stars [8,24–35]. In particular, at a high density of a neutron star and heavy ion collisions, the proton fraction of β-stable matter may increase and the splitting of the effective mass should affect the transfer properties. Hence, the isovector-scalar meson is taken into account, while its individual contribution is small in the NN interaction due toits heavy mass ($\sim$980 MeV, more than the nucleon mass). But for the highly asymmetric system, the total contribution of the δ meson cannot be ignored.

The relativistic treatment of the quantum hadrodynamic (QHD) models automatically includes the spin-orbit force, the finite range, and the density dependence of the nuclear interaction. The relativistic mean field (RMF), or the E-RMF model, has the advantage that, with the proper relativistic kinematics and with the meson properties already known or fixed from the properties of a small number of finite nuclei, it gives excellent results for binding energies, root-mean-square (rms) radii, quadrupole and hexadecapole deformations, and other properties of spherical and deformed nuclei [36–40]. The quality of the results is comparable to that found in nonrelativistic nuclear structure calculations with effective Skyrme [41] or Gogny [42] forces.

The theory and equations for finite nuclei and nuclear matter can be found in Refs. [1,2,43,44] and we shall give only the outline of the formalism. We start from Ref. [1] where the field equations are derived from an energy density functional containing Dirac baryons and classical scalar and vector mesons. The field equations for mesons and nucleons are solved by the self-consistent way, which is a very strong technique in effective field theory. It gives excellent results for finite and infinite nuclear systems [13,44–48]. The energy density functional for finite nuclei can be written as [2,43,44]

$$
\begin{aligned}
\mathcal{E}(r) = \sum_{\alpha} \varphi_{\alpha}^{\dagger}(r)\Bigg\{ -i\boldsymbol{\alpha}\cdot\nabla + \beta[M - \Phi(r) - \tau_3 D(r)] + W(r) + \frac{1}{2}\tau_3 R(r) + \frac{1+\tau_3}{2}A(r) - \frac{i\beta\boldsymbol{\alpha}}{2M}\cdot\Bigg(f_v \nabla W(r) \\
+ \frac{1}{2} f_\rho \tau_3 \nabla R(r)\Bigg)\Bigg\}\varphi_{\alpha}(r) + \left(\frac{1}{2} + \frac{\kappa_3}{3!}\frac{\Phi(r)}{M} + \frac{\kappa_4}{4!}\frac{\Phi^2(r)}{M^2}\right)\frac{m_s^2}{g_s^2}\Phi^2(r) - \frac{\zeta_0}{4!}\frac{1}{g_v^2}W^4(r) + \frac{1}{2g_s^2}\left(1 + \alpha_1\frac{\Phi(r)}{M}\right)(\nabla\Phi(r))^2 \\
- \frac{1}{2g_v^2}\left(1 + \alpha_2\frac{\Phi(r)}{M}\right)(\nabla W(r))^2 - \frac{1}{2}\left(1 + \eta_1\frac{\Phi(r)}{M} + \frac{\eta_2}{2}\frac{\Phi^2(r)}{M^2}\right)\frac{m_v^2}{g_v^2}W^2(r) - \frac{1}{2e^2}(\nabla A(r))^2 - \frac{1}{2g_\rho^2}(\nabla R(r))^2 \\
- \frac{1}{2}\left(1 + \eta_\rho\frac{\Phi(r)}{M}\right)\frac{m_\rho^2}{g_\rho^2}R^2(r) - \Lambda_v(R^2(r)\times W^2(r)) + \frac{1}{2g_\delta^2}(\nabla D(r))^2 - \frac{1}{2}\frac{{m_\delta}^2}{g_\delta^2}(D^2(r)),
\end{aligned} \tag{1}
$$

where Φ, W, R, D, and A are the fields for σ,ω,ρ,δ, and the photon, and g_σ, g_ω, g_ρ, g_δ, and $\frac{e^2}{4\pi}$ are their coupling constant, and their masses are m_σ, m_ω, m_ρ, and m_δ, respectively. In the energy functional, the nonlinearity as well as the cross-coupling up to a maximum of fourth order is taken into account. This is restricted due the condition $1 \geqslant \frac{\text{field}}{M}$ (M = nucleon mass) and the nonsignificant contribution of the higher order [4]. The higher nonlinear coupling for ρ- and δ-meson fields are not taken in the energy functional, because the expectation values of the ρ and δ fields are an order of magnitude less than that of the ω field and they have only marginal contribution to finite nuclei. For example, in calculations of the high-density equation of state, Müller and Serot [43] find the effects of a quartic ρ meson coupling (R^4) to be appreciable only in stars made of pure neutron matter. A surface contribution $-\alpha_3\Phi\,(\nabla R)^2/(2g_\rho^2 M)$ is tested in Ref. [49] and it is found to have absolutely negligible effects. We should note, nevertheless, that very recently it has been shown that couplings of the type $\Phi^2 R^2$ and $W^2 R^2$ are useful to modify the neutron radius in heavy nuclei while making very small changes to the proton radius and the binding energy [10].

The Dirac equation corresponding to the energy density equation (1) becomes

$$
\left\{-i\boldsymbol{\alpha}\cdot\nabla + \beta[M - \Phi(r) - \tau_3 D(r)] + W(r) + \frac{1}{2}\tau_3 R(r) + \frac{1+\tau_3}{2}A(r) - \frac{i\beta\boldsymbol{\alpha}}{2M}\cdot\left[f_v\nabla W(r) + \frac{1}{2}f_\rho\tau_3\nabla R(r)\right]\right\}\varphi_\alpha(r) = \varepsilon_\alpha\,\varphi_\alpha(r). \tag{2}
$$

The mean field equations for Φ, W, R, D, and A are given by

$$-\Delta\Phi(r)+m_s^2\Phi(r)=g_s^2\rho_s(r)-\frac{m_s^2}{M}\Phi^2(r)\left(\frac{\kappa_3}{2}+\frac{\kappa_4}{3!}\frac{\Phi(r)}{M}\right)+\frac{g_s^2}{2M}\left(\eta_1+\eta_2\frac{\Phi(r)}{M}\right)\frac{m_v^2}{g_v^2}W^2(r)+\frac{\eta_\rho}{2M}\frac{g_s^2}{g_\rho{}^2}m_\rho^2R^2(r)$$
$$+\frac{\alpha_1}{2M}[(\nabla\ \Phi(r))^2+2\Phi(r)\Delta\Phi(r)]+\frac{\alpha_2}{2M}\frac{g_s^2}{g_v^2}(\nabla\ W(r))^2, \tag{3}$$

$$-\Delta W(r)+m_v^2W(r)=g_v^2\left(\rho(r)+\frac{f_v}{2}\rho_{\mathrm{T}}(r)\right)-\left(\eta_1+\frac{\eta_2}{2}\frac{\Phi(r)}{M}\right)\frac{\Phi(r)}{M}m_v^2W(r)-\frac{1}{3!}\zeta_0W^3(r)$$
$$+\frac{\alpha_2}{M}[\nabla\ \Phi(r)\cdot\nabla\ W(r)+\Phi(r)\Delta W(r)]-2\Lambda_vg_v{}^2R^2(r)W(r), \tag{4}$$

$$-\Delta R(r)+m_\rho^2R(r)=\frac{1}{2}g_\rho^2\left(\rho_3(r)+\frac{1}{2}f_\rho\rho_{\mathrm{T},3}(r)\right)-\eta_\rho\frac{\Phi(r)}{M}m_\rho^2R(r)-2\ \Lambda_vg_\rho{}^2R(r)W^2(r), \tag{5}$$

$$-\Delta A(r)=e^2\rho_{\mathrm{p}}(r), \tag{6}$$

$$-\Delta D(r)+m_\delta{}^2D(r)=g_\delta^2\rho_{s3}, \tag{7}$$

where the baryon, scalar, isovector, proton, and tensor densities are

$$\rho(r)=\sum_\alpha\varphi_\alpha^\dagger(r)\varphi_\alpha(r)\,, \tag{8}$$

$$\rho_s(r)=\sum_\alpha\varphi_\alpha^\dagger(r)\beta\varphi_\alpha(r)\,, \tag{9}$$

$$\rho_3(r)=\sum_\alpha\varphi_\alpha^\dagger(r)\tau_3\varphi_\alpha(r)\,, \tag{10}$$

$$\rho_{\mathrm{p}}(r)=\sum_\alpha\varphi_\alpha^\dagger(r)\left(\frac{1+\tau_3}{2}\right)\varphi_\alpha(r), \tag{11}$$

$$\rho_{\mathrm{T}}(r)=\sum_\alpha\frac{i}{M}\nabla\cdot[\varphi_\alpha^\dagger(r)\beta\boldsymbol{\alpha}\ \varphi_\alpha(r)], \tag{12}$$

$$\rho_{\mathrm{T},3}(r)=\sum_\alpha\frac{i}{M}\nabla\cdot[\varphi_\alpha^\dagger(r)\beta\boldsymbol{\alpha}\ \tau_3\varphi_\alpha(r)], \tag{13}$$

$$\rho_{s3}(r)=\sum_\alpha\varphi_\alpha^\dagger(r)\tau_3\beta\varphi_\alpha(r), \tag{14}$$

with $\rho_{s3}=\rho_{sp}-\rho_{sn}$, ρ_{sp} and ρ_{sn} are scalar densities for the proton and neutron, respectively. The scalar density ρ_s is expressed as the sum of the proton (p) and neutron (n) densities $\rho_s=\langle\psi\psi\rangle=\rho_{sp}+\rho_{sn}$, which are given by

$$\rho_{si}=\frac{2}{(2\pi)^3}\int_0^{k_i}d^3k\frac{M_i^*}{\left(k^2+M_i^{*2}\right)^{\frac{1}{2}}},\quad i=p,n. \tag{15}$$

k_i is the nucleon's Fermi momentum and M_p^*, M_n^* are the proton and neutron effective masses, respectively, and can be written as

$$M_p^*=M-\Phi(r)-D(r), \tag{16}$$

$$M_n^*=M-\Phi(r)+D(r). \tag{17}$$

Thus, the δ field splits the nucleon effective masses. The baryon density is given by

$$\rho_B=\langle\psi\gamma^0\psi\rangle=\gamma\int_0^{k_F}\frac{d^3k}{(2\pi)^3}, \tag{18}$$

where γ is spin or isospin multiplicity ($\gamma=4$ for symmetric nuclear matter and $\gamma=2$ for pure neutron matter). The proton and neutron Fermi momentum will also split, while they have to fulfill the following condition:

$$\rho_B=\rho_p+\rho_n$$
$$=\frac{2}{(2\pi)^3}\int_0^{k_p}d^3k+\frac{2}{(2\pi)^3}\int_0^{k_n}d^3k. \tag{19}$$

Because of the uniformity of the nuclear system for infinite nuclear matter all of the gradients of the fields in Eqs. (3)–(7) vanish and only the κ_3, κ_4, η_1, η_2, and ζ_0 nonlinear couplings remain. Due to the fact that the solution of symmetric nuclear matter in a mean field depends on the ratios g_s^2/m_s^2 and g_v^2/m_v^2 [50], we have seven unknown parameters. By imposing the values of the saturation density, total energy, incompressibility modulus, and effective mass, we still have three free parameters (the value of g_ρ^2/m_ρ^2 is fixed from the bulk symmetry energy coefficient J). The energy density and pressure of nuclear matter are given by

$$\epsilon=\frac{2}{(2\pi)^3}\int d^3kE_i^*(k)+\rho W$$
$$+\frac{m_s^2\Phi^2}{g_s^2}\left(\frac{1}{2}+\frac{\kappa_3}{3!}\frac{\Phi}{M}+\frac{\kappa_4}{4!}\frac{\Phi^2}{M^2}\right)$$
$$-\frac{1}{2}m_v^2\frac{W^2}{g_v^2}\left(1+\eta_1\frac{\Phi}{M}+\frac{\eta_2}{2}\frac{\Phi^2}{M^2}\right)-\frac{1}{4!}\frac{\zeta_0W^4}{g_v^2}+\frac{1}{2}\rho_3R$$
$$-\frac{1}{2}\left(1+\frac{\eta_\rho\Phi}{M}\right)\frac{m_\rho^2}{g_\rho^2}R^2-\Lambda_vR^2\times W^2+\frac{1}{2}\frac{m_\delta^2}{g_\delta^2}(D^2), \tag{20}$$

$$P=\frac{2}{3(2\pi)^3}\int d^3k\frac{k^2}{E_i^*(k)}-\frac{m_s^2\Phi^2}{g_s^2}\left(\frac{1}{2}+\frac{\kappa_3}{3!}\frac{\Phi}{M}+\frac{\kappa_4}{4!}\frac{\Phi^2}{M^2}\right)$$
$$+\frac{1}{2}m_v^2\frac{W^2}{g_v^2}\left(1+\eta_1\frac{\Phi}{M}+\frac{\eta_2}{2}\frac{\Phi^2}{M^2}\right)+\frac{1}{4!}\frac{\zeta_0W^4}{g_v^2}$$
$$+\frac{1}{2}\left(1+\frac{\eta_\rho\Phi}{M}\right)\frac{m_\rho^2}{g_\rho^2}R^2+\Lambda_vR^2\times W^2-\frac{1}{2}\frac{m_\delta^2}{g_\delta^2}(D^2), \tag{21}$$

where $E_i^*(k) = \sqrt{k^2 + M_i^{*2}}$ $(i = p,n)$. In the context of density functional theory, it is possible to parametrize the exchange and correlation effects through local potentials (Kohn-Sham potentials), as long as those contributions are small enough [51]. The Hartree values are the ones that control the dynamics in the relativistic Dirac-Brückner-Hartree-Fock (DBHF) calculations. Therefore, the local meson fields in the RMF formalism can be interpreted as Kohn-Sham potentials and, in this sense, Eqs. (2)–(7) include effects beyond the Hartree approach through the nonlinear couplings [1,2,44].

III. RESULTS AND DISCUSSIONS

Our calculated results are shown in Figs. 1–10 and Table I for both finite nuclei and infinite nuclear matter systems. The effect of the δ meson and the crossed coupling constant Λ_v of the ω-ρ fields on some selected nuclei, such as ^{48}Ca and ^{208}Pb, are demonstrated in Figs. 1–4 and the nuclear matter outcomes are displayed in rest of the figures and Table I. In one of our recent publications [11], the explicit dependence of $\Lambda_v(\omega - \rho)$ on nuclear matter properties is shown and it is found that it has a significant implication on various physical properties, such as the mass and radius of a neutron star and $E_{\rm sym}$ asymmetry energy and its slope parameter $L_{\rm sym}$ for infinite nuclear matter at high densities. Here, only the influence of Λ_v on finite nuclei and that of g_δ on both finite and infinite nuclear systems are studied.

A. Selection of g_δ, g_ρ, and Λ_v

The G2 set is a phenomenological parametrization. All the parameters in this set are adjusted to reproduce some specific experimental data. Therefore, each of the coupling constant contains physics and it is difficult to disentangle the influence of the various physical properties on these parameters. Apart from this, all the parameters depend on the underlying fitting strategy. Thus we cannot just add one more parameter like g_δ to study its effect keeping all the other parameters of G2 fixed. This is because the physics described by this g_δ might already be included in the other parameters and leading towards a double counting. Since both g_δ and g_ρ depend on the isospin symmetry, we expect that some parts of the effects of g_δ might be taken into account in the parameter g_ρ at the time of the fitting of the G2 set. Fortunately, in this particular case of g_δ, we expect a connection between the parameters g_δ and g_ρ as both of them carry isospin. In such a situation, there are two possible solutions to this problem: (i) the dependence on both g_δ and g_ρ independently, in this case, modify the parameter g_ρ to fit an experimental data which is linked to both g_ρ and g_δ for each new given value of g_δ, such as the binding energy or (ii) get a completely new parameter set as it is done for G2 including the δ meson as a degree of freedom from the beginning, i.e., start from *ab initio* calculations as done in [52].

Here, we study the effect of g_δ on finite and infinite nuclear matter systems adopting the first approach. The combination of g_δ and g_ρ are chosen in such a way that for a given value of g_δ, the combined values of g_δ and g_ρ on top of G2 (with changed g_ρ) reproduce the physical observable of a particular

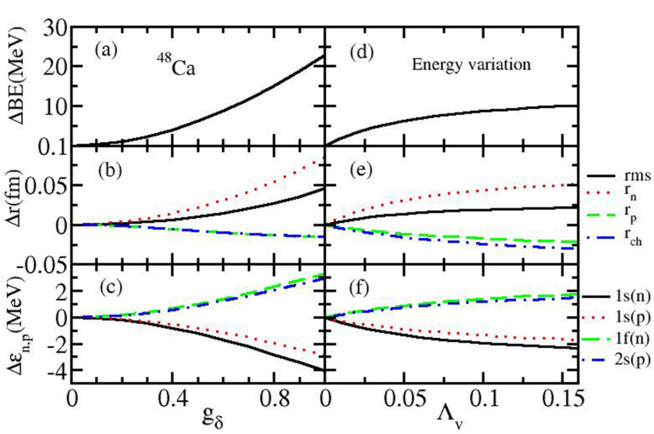

FIG. 1. (Color online) Binding energy (BE), root mean square radius, and first $(1s^{n,p})$ and last $(1f^n, 2s^p)$ occupied orbits for ^{48}Ca using various $(g_\rho, g_\delta, \Lambda_v)$ combinations of Table I.

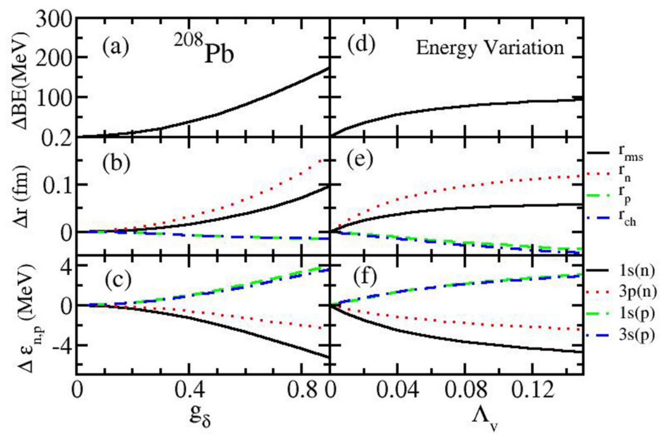

FIG. 2. (Color online) Same as Fig. 1 for ^{208}Pb.

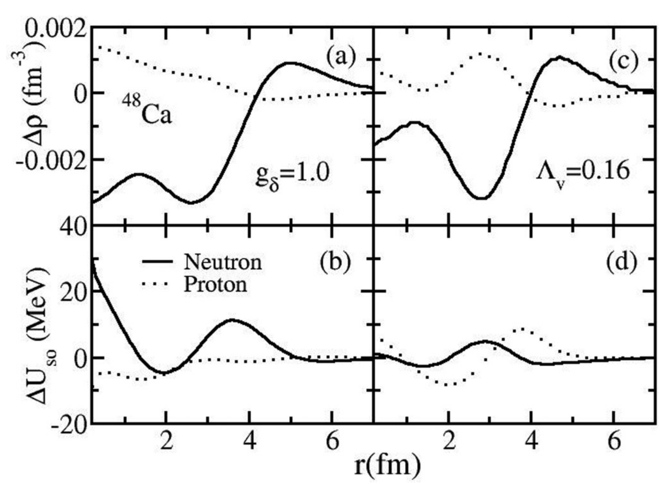

FIG. 3. The neutron and proton density with radial coordinate r(fm) at different combinations of $(g_\rho,\ g_\delta)$ in (a) and with Λ_v in (c). The variation of spin-orbit potential for proton and neutron are shown in (b) and (d) by keeping the same g_δ and Λ_v as (a) and (c), respectively.

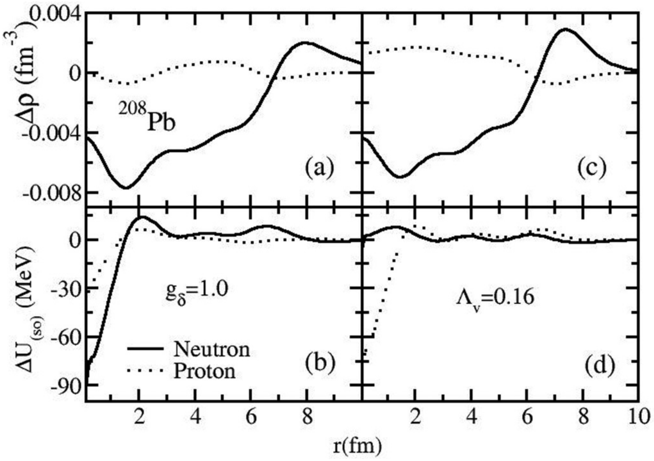

FIG. 4. Same as Fig. 3 for ^{208}Pb.

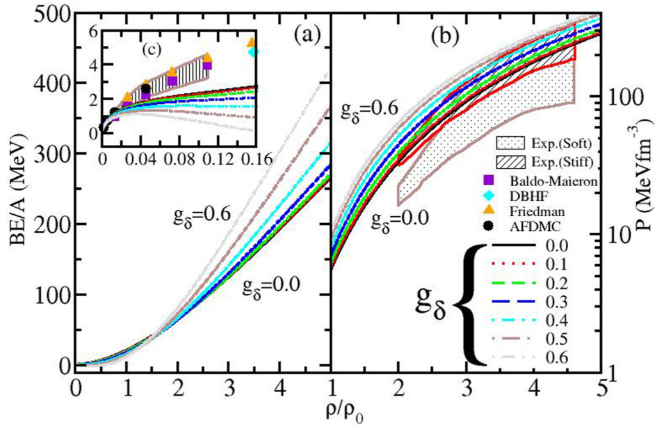

FIG. 6. (Color online) Energy per particle and pressure density with respect to baryon density at various combinations of g_δ from Table I.

experimental measure. In this case, we have taken the binding energies of ^{48}Ca and ^{208}Pb as the experimental data. These values change from their original prediction of G2 with the addition of a given g_δ. To bring back the G2 binding energies of ^{48}Ca and ^{208}Pb, we modified the g_ρ coupling. This is due to the isospin coupling being linked with both g_δ and g_ρ. In this way, we get various combinations of (g_ρ, g_δ) for different given value of g_δ. The combination of g_ρ and g_δ are listed in Table I which are used in the calculations for both finite nuclei and infinite nuclear matter. It is to be noted that while setting the g_δ-g_ρ combination, the Λ_v is taken as zero. On the other hand, Λ_v changes on top of the pure G2 parameter set to see the influence of Λ_v for finite nuclei, as the binding energy and proton radius r_p are almost insensitive to Λ_v [53].

B. Finite nuclei

In this section, we analyzed the effects of the δ meson and Λ_v couplings in finite nuclei. For this, we calculate the binding energy (BE), root mean square neutron (r_n), proton (r_p), charge (r_{ch}), and matter radius ($r_{\rm rms}$), and energy of first- and last-filled orbitals of ^{48}Ca and ^{208}Pb with various g_δ and Λ_v. The finite size of the nucleon is taken into account for the charge radius using the relation $r_{ch} = \sqrt{r_p^2 + 0.64}$. The results are shown in Figs. 1 and 2.

When we analyze the effect of g_δ, we keep $\Lambda_v = 0$ and vice versa. In Fig. 1(a), we have shown the binding energy difference ΔBE of ^{48}Ca between the two solutions obtained with ($g_\rho, g_\delta = 0$) and (g_ρ, g_δ), i.e.,

$$\Delta \mathrm{BE} = \mathrm{BE}(g_\rho, g_\delta = 0) - \mathrm{BE}(g_\rho, g_\delta). \tag{22}$$

Here BE($g_\rho, g_\delta = 0$) is the binding energy at $g_\delta = 0$ in the adjusted combination of (g_ρ, g_δ) and BE(g_ρ, g_δ) is the binding energy with nonzero g_ρ and g_δ combined which reproduce the same binding of pure G2. Thus, the contribution of the δ meson to the binding energy is obtained from this ΔBE. Similarly, the effect of the δ meson in the radius of finite nuclei is seen

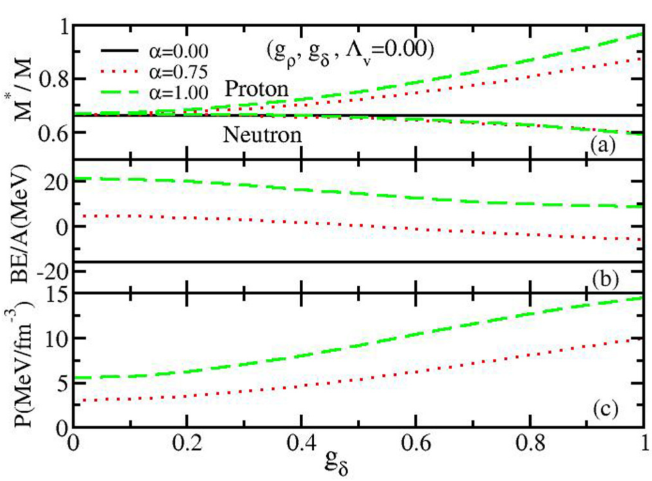

FIG. 5. (Color online) Variation of nucleonic effective masses, binding energy per particle (BE/A) and pressure density as a function of g_δ on the saturation density of the G2 parameter set for nuclear matter.

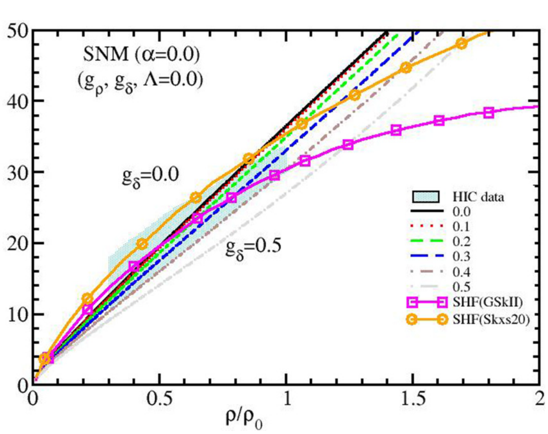

FIG. 7. (Color online) Symmetry energy $E_{\rm sym}$ (MeV) of symmetric nuclear matter with respect to density by taking different value of g_δ sets. The heavy ion collision (HIC) experimental data [63] (shaded region) and nonrelativistic Skyrme GSkII [64] and Skxs20 [65] predictions are also given. $\Lambda_v = 0.0$ is taken.

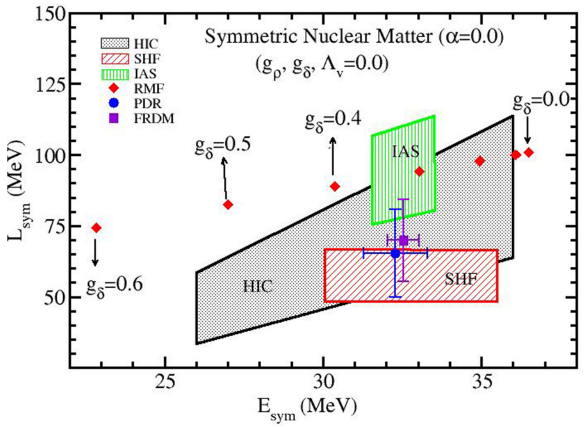

FIG. 8. (Color online) Constraints on E_{sym} with its first derivative, L_{sym}, at saturation density for symmetric nuclear matter. The experimental results of HIC [63], PDR [70,71], and IAS [72] are given. The theoretical prediction of the finite range droplet model (FRDM) and Skyrme parametrization are also given [73], SHF [59].

from

$$\Delta r = r(g_\rho, g_\delta = 0) - r(g_\rho, g_\delta), \tag{23}$$

where $r(g_\rho, g_\delta = 0)$ is the radius at $g_\delta = 0$ in the adjusted (g_ρ, g_δ) and $r(g_\rho, g_\delta)$ is the G2 radius after reshuffling the g_ρ and g_δ combination. The Δr with corresponding g_δ for ^{48}Ca is shown in Fig. 1(b). We have adopted the same scheme to estimate the effect of the δ meson on the first and last occupied levels, which are shown in Fig. 1(c). It is given as

$$\Delta\epsilon = \epsilon(g_\rho, g_\delta = 0) - \epsilon(g_\rho, g_\delta), \tag{24}$$

where $\epsilon(g_\rho, g_\delta = 0)$ is the single-particle energy at $(g_\rho\ g_\delta = 0)$ combination, g_ρ is not the same as the G2 set and $\epsilon(g_\rho, g_\delta)$ is the energy of the occupied level with different values of g_ρ and g_δ sets.

The effects of Λ_v coupling on ^{48}Ca properties such as binding energy, radius, and single-particle energy of the first and last occupied levels are shown in the second column

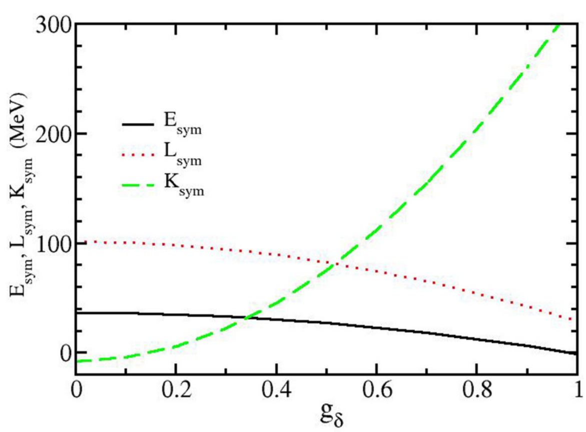

FIG. 9. (Color online) Symmetry energy E_{sym} (MeV), slope coefficients L_{sym} (MeV), and K_{sym} (MeV) at different sets of g_ρ and g_δ as given in Table I with $\Lambda_v = 0.0$.

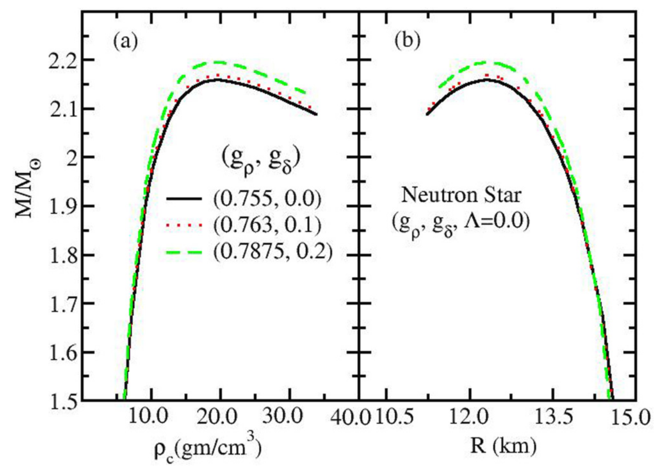

FIG. 10. (Color online) The mass and radius of a neutron star at different values of g_δ. (a) $M/M_\odot$ with neutron star density (gm/cm^3), (b) $M/M_\odot$ with neutron star radius (km).

of Fig. 1. Here, we have taken $g_\delta = 0$. Following the same procedure of g_δ to evaluate ΔBE, Δr, and $\Delta\epsilon$, we estimate the contributions of Λ_v on the physical quantities. The variation of binding energy (ΔBE) with Λ_v can be written as

$$\Delta\mathrm{BE} = \mathrm{BE}(G2) - \mathrm{BE}(G2 + \Lambda_v), \tag{25}$$

where BE($G2$) is the binding energy with pure G2 set and BE($G2 + \Lambda_v$) is for G2 with additional ω-ρ cross coupling. The changes in the radius with Λ_v is given by

$$\Delta r = r(G2) - r(G2 + \Lambda_v), \tag{26}$$

where $r(G2)$ is the radius of ^{48}Ca with pure G2 and $r(G2 + \Lambda_v)$ with additional Λ_v on top of pure G2. This results are shown in Fig. 1(e). The effect of Λ_v on the first- and last-filled single-particle levels are given in Fig. 1(f) using

$$\Delta\epsilon = \epsilon(\mathrm{G2}) - \epsilon(\mathrm{G2} + \Lambda_v), \tag{27}$$

where ϵ(G2) is the single-particle energy of the first and last occupied levels of ^{48}Ca with original G2 and $\epsilon(\mathrm{G2} + \Lambda_v)$ at various Λ_v values on top of the G2 parameter set. Similar to ^{48}Ca, we have repeated the calculations for ^{208}Pb in Fig. 2 to

TABLE I. The symmetry energy E_{sym} (MeV), slope coefficient L_{sym} (MeV), and K_{sym} (MeV) at different sets of (g_ρ, g_δ).

(g_ρ, g_δ)	E_{sym}	L_{sym}	K_{sym}
(0.755, 0.0)	36.48	100.91	−7.57
(0.763, 0.1)	36.08	100.11	−4.25
(0.7875, 0.2)	34.94	97.88	5.68
(0.827, 0.3)	33.05	94.21	22.21
(0.879, 0.4)	30.38	89.01	45.37
(0.9423, 0.5)	26.99	82.45	75.10
(1.0142, 0.6)	22.84	74.40	111.45
(1.0937, 0.7)	17.98	65.02	154.36
(1.179, 0.8)	12.39	54.24	203.85
(1.2691, 0.9)	6.09	42.10	259.91
(1.3634, 1.0)	−0.89	28.71	322.51

study the effect of g_δ and Λ_v. We have followed exactly the same method as that of ^{48}Ca and calculated the variation in binding energy, radii, and single-particle levels. We obtained almost similar results to those of Fig. 1.

From the figures (Figs. 1 and 2), it is evident that the binding energy, radii, and single particle levels $\epsilon_{n,p}$ affected drastically with g_δ contrary to the effect of Λ_v. A careful inspection shows a slight decrease of r_n with the increase of Λ_v consistent with the analysis of [53]. Again, it is found that the binding energy increases with an increase of the coupling strength up to $g_\delta \sim 1.1$ and no convergence solution available beyond this value. Similar to the g_δ limit, there is a limit for $\Lambda_v \sim 0.16$ also, beyond which no solution exists. From the anatomy of g_δ on r_n and r_p (or Δr), we find their opposite trend in size. That means the value of r_n decreases and r_p increases with g_δ for both ^{48}Ca and ^{208}Pb. This interesting result may help us to settle the charge radius anomaly of ^{40}Ca and ^{48}Ca.

In Figs. 1(c) and 1(f), we have shown the change in single-particle energy $\Delta\epsilon_{n,p}$ of the first $(1s^{n,p})$ and last $(1f^n$ and $2s^p)$ filled orbitals for ^{48}Ca as a function of g_δ and Λ_v, respectively. The effect of Λ_v is marginal, i.e., almost negligible on $\epsilon_{n,p}$ orbitals which is given in Fig. 1(f). However, this is significant with the increasing value of g_δ. We also get a similar trend for ^{208}Pb, which is shown in Fig. 2(c). In both the representative cases, we notice orbital shifting only for the last-filled levels (for $g_\delta \geqslant 1.0$, not shown in the figure).

The change in nucleon density $\Delta\rho$ distribution (proton ρ_p and neutron ρ_n) and spin orbit interaction potential ΔU_{so} for finite nuclei are shown in Figs. 3 and 4. The calculations are done with one set of (g_ρ, g_δ) for checking the effect of g_δ in finite nuclei, and shown in Figs. 3(a) and 3(b) for ^{48}Ca. Here, we have taken $g_\delta = 1.0$ and corresponding modified $g_\rho = 1.3634$ for calculating the $\Delta\rho$ $[\rho(g_\rho = 1.3634, g_\delta = 0) - \rho(g_\rho = 1.3634, g_\delta = 1.0)]$ and $\Delta U_{so}[U_{so}(g_\rho = 1.3634, g_\delta = 0) - U_{so}(g_\rho = 1.3634, g_\delta = 1.0)]$. To see the effectiveness of Λ_v on the nucleon distribution and spin orbit interaction potential, we have estimated the $\Delta\rho[\rho(G2) - \rho(G2 + \Lambda_v = 0.16)]$ and $\Delta U_{so}[U_{so}(G2) - U_{so}(G2 + \Lambda_v = 0.16)]$ for both neutron and proton, respectively. The results are shown in Figs. 3(c) and 3(d). Similarly, we have given these observables for ^{208}Pb in Fig. 4. It is clear from this analysis that the coupling strengths of the δ meson and the isoscalar-vector and isovector-vector cross couplings are quite influential for the density and spin-orbit interaction. This effect is mostly confined to the central and intermediate region of the nucleus.

C. Nuclear matter

In this section, we calculate nuclear matter properties, such as energy and pressure densities, symmetry energy, radius and mass of the neutron star using ω-ρ and δ couplings on top of the G2 parametrization. As mentioned earlier, the ω-ρ cross coupling plays a vital role for nuclear matter systems, a detailed account is available in Ref. [11]. The main aim of this section is to take the δ meson as an additional degree of freedom in our calculations and elaborate on the effect of the nuclear matter system within the G2 parameter set. In a highly asymmetric system, such as the neutron star and supernova explosion, the contribution of the δ meson is important. This is because of the high asymmetry due to the isospin as well as the difference in neutron and proton masses. Here, in the calculations, the β equilibrium and charge neutrality conditions are not considered. We only vary the neutron and proton components with an asymmetry parameter α, defined as $\alpha = \frac{\rho_n - \rho_p}{\rho_n + \rho_p}$. The splitting in nucleon masses is evident from Eqs. (16) and (17) due to the inclusion of the isovector scalar δ meson. For $\alpha = 0.0$, the nuclear matter system is purely symmetrical and for other nonzero values of α, the system gets more and more asymmetric. For $\alpha = 1.0$, it is a case of pure neutron matter. In Fig. 5(a), the effective masses of the proton and neutron are given as a function of g_δ. As we have mentioned, the δ meson is responsible for the splitting of effective masses [Eqs. (16) and (17)], this splitting increases continuously with coupling strength g_δ. In Fig. 5, the splitting is shown for a few representative cases at $\alpha = 0.0$, 0.75, and 1.0. The solid line is for $\alpha = 0.0$ and $\alpha = 0.75$, 1.0 are shown by dotted and dashed lines, respectively. From the figure, it is clear that the effective mass is unaffected by symmetric matter. The proton effective mass M_p^* is above the reference line with $\alpha = 0$ and the neutron effective mass always lies below it. The effect of g_δ on the binding energy per nucleon is shown in Fig. 5(b) and pressure density in Fig. 5(c). One can easily see the effect of the δ-meson interaction on the energy and pressure density of the nuclear system. The energy and pressure density show opposite trends to each other with the increase of g_δ.

D. Energy and pressure density

We analyze the binding energy per nucleon and pressure density including the contribution of the δ meson in the G2 Lagrangian as a function of density. As was mentioned earlier, the addition of the δ meson is due to its importance on asymmetric nuclear matter as well as to make a fully fledged E-RMF model. This is tested by calculating the observables at different values of the δ-meson coupling strength g_δ. In Fig. 6, we show the calculated BE$/A$ and $\mathcal{P}$ for pure neutron matter $(\alpha = 1.0)$ with baryonic density for different combinations of g_ρ and g_δ values, which is shown in the first column in Table I.

It is seen from Fig. 6(a) that the binding increases with g_δ in the lower density region and in the higher density region, the binding energy curve for finite g_δ crosses the curve of $g_\delta = 0.0$. The EOS with the δ meson is stiffer than the one with a pure G2 set at higher density. As a result, one will get a heavier mass for the neutron star, which agrees with the present experimental finding [54]. For a comparison of the data at lower density (dilute system, $0 < \rho/\rho_0 < 0.16$), the zoomed version of the region is shown as an inset Fig. 6(c) inside Fig. 6(a). From the zoomed inset portion, it is clearly seen that the curves with various g_δ at $\alpha = 1.0$ (pure neutron matter) deviate from other theoretical predictions, such as Baldo-Maieron [55], DBHF [56], Friedman [57], auxiliary-field diffusion Monte Carlo (AFDMC) [58], and Skyrme interaction [59]. This is an inherited problem from the RMF or E-RMF formalisms, which needs more theoretical attention. Similarly, the pressure density for different sets of (g_ρ, g_δ) are given in Fig. 6(b). At high density we can easily see that the curve becomes stiffer with the coupling strength g_δ. The experimental constraint of the equation of state obtained from heavy ion flow data for both stiff and soft EOS is also displayed for comparison in the region $2 < \rho/\rho_0 < 4.6$ [60]. Our results match with the stiff EOS data of Ref. [60].

E. Symmetry energy

The symmetric energy $E_{\rm sym}$ is important in infinite nuclear matter and finite nuclei, because of isospin dependence in the interaction. The isospin asymmetry arises due to the difference in densities and masses of the neutron and proton, respectively. The density type of isospin asymmetry is taken care of by the ρ meson (isovector-vector meson) and mass asymmetry by the δ meson (isovector-scalar meson). The expression of symmetry energy $E_{\rm sym}$ is a combined expression of ρ and δ mesons, which is defined as [4,8,61,62]

$$E_{\rm sym}(\rho) = E_{\rm sym}^{\rm kin}(\rho) + E_{\rm sym}^{\rho}(\rho) + E_{\rm sym}^{\delta}(\rho), \tag{28}$$

with

$$E_{\rm sym}^{\rm kin}(\rho) = \frac{k_F^2}{6E_F^*}; \quad E_{\rm sym}^{\rho}(\rho) = \frac{g_\rho^2 \rho}{8m_\rho^{*2}} \tag{29}$$

and

$$E_{\rm sym}^{\delta}(\rho) = -\frac{1}{2}\rho\frac{g_\delta^2}{m_\delta^2}\left(\frac{M^*}{E_F}\right)^2 u_\delta\left(\rho, M^*\right). \tag{30}$$

The last function u_δ is from the discreteness of the Fermi momentum. This momentum is quite large in the nuclear matter system and can be treated as a continuum and continuous system. The function u_δ is defined as

$$u_\delta(\rho, M^*) = \frac{1}{1 + 3\frac{g_\delta^2}{m_\delta^2}}\left(\frac{\rho^s}{M^*} - \frac{\rho}{E_F}\right). \tag{31}$$

In the limit of the continuum, the function $u_\delta \approx 1$. The whole symmetry energy ($E_{\rm sym}^{\rm kin} + E_{\rm sym}^{\rm pot}$) arises from ρ and δ mesons and is given as

$$E_{\rm sym}(\rho) = \frac{k_F^2}{6E_F^*} + \frac{g_\rho^2 \rho}{8m_\rho^{*2}} - \frac{1}{2}\rho\frac{g_\delta^2}{m_\delta^2}\left(\frac{M^*}{E_F}\right)^2 u_\delta(\rho, M^*), \tag{32}$$

where the effective energy $E_F^* = \sqrt{(k_F^2 + M^{*2})}$, k_F is the Fermi momentum. The effective mass of the ρ meson is modified, because of the cross coupling of ρ-ω and is given by

$$m_\rho^{*2} = \left(1 + \eta_\rho\frac{\Phi}{M}\right)m_\rho^2 + 2g_\rho^2(\Lambda_v W^2). \tag{33}$$

The cross coupling of isoscalar-isovector mesons (Λ_v) modified the density dependence of $E_{\rm sym}$ without affecting the saturation properties of the symmetric nuclear matter (SNM). This is explained explicitly in Ref. [11] so there is no need for special attention here. In the E-RMF model with a pure G2 set, the symmetric nuclear matter saturates at $\rho_0 = 0.153\ {\rm fm}^{-3}$, ${\rm BE}/A = 16.07$ MeV, compressibility $K_0 = 215$ MeV, and symmetry energy of $E_{\rm sym} = 36.42$ MeV [1,2].

In the numerical calculation, the coefficient of symmetry energy $E_{\rm sym}$ is obtained by the energy difference of symmetric and pure neutron matter at saturation and it is defined by Eq. (32) for a quantitative description at various densities. Our results for $E_{\rm sym}$ are shown in Fig. 7 with experimental heavy ion collision (HIC) data [63] and other theoretical predictions of the nonrelativistic Skyrme-Hartree-Fock model. The calculation is done for symmetric nuclear matter with different values of g_δ, which are compared with two selective force parameter sets GSkII [64] and Skxs20 [65]. For more discussion one can see Ref. [59], where 240 different Skyrme parametrizations are used. Here in our calculation, as usual $\Lambda_v = 0$ to see the effect of δ-meson coupling on $E_{\rm sym}$. In this figure, the shaded region represents the HIC data [63] within the $0.3 < \rho/\rho_0 < 1.0$ region and the square and circle symbols represent the SHF results for GSkII and Skxs20, respectively. Analyzing Fig. 7, the $E_{\rm sym}$ of G2 matches with the shaded region in the low density region, however as the density increases, the value of $E_{\rm sym}$ moves away. Again, the symmetry energy becomes softer by increasing the value of coupling strength g_δ. For a higher value of g_δ, again the curve moves far from the empirical shaded area. In this way, we can fix the limiting constraint on the coupling strength of the δ meson and nucleon. This constraint may help to improve the G2 + g_δ parameter set for both finite and infinite nuclear systems. It is important to note that the EOS and also the symmetry energy are calculated in Ref. [62]. Analyzing the results of the EOS with the DD-ME2 and DD-MEδ parametrizations, we find that DD-ME2 overestimates the data, while DD-MEδ matches well. On the other hand the symmetry energy with these sets coincides up to $2\rho_0$ of the nuclear matter density. From this result, we cannot isolate the contribution of the δ meson on $E_{\rm sym}$ or EOS, because the goal of the two parametrizations is to reproduce the data. However, in our present case, our aim is to entangle the contribution of the δ meson with and without g_δ coupling keeping all other parameters intact.

The symmetry energy of a nuclear system is a function of baryonic density ρ, hence it can be expanded in a Taylor series around the saturation density ρ_0 as Eq. (32):

$$E_{\rm sym}(\rho) = E_0 + L_{\rm sym}\mathcal{Y} + \tfrac{1}{2}K_{\rm sym}\mathcal{Y}^2 + O[\mathcal{Y}^3], \tag{34}$$

where $E_0 = E_{\rm sym}(\rho = \rho_0)$, $\mathcal{Y} = \frac{\rho - \rho_0}{3\rho_0}$, and the coefficients $L_{\rm sym}$ and $K_{\rm sym}$ are defined as

$$L_{\rm sym} = 3\rho\left(\frac{\partial E_{\rm sym}}{\partial\rho}\right)_{\rho=\rho_0}, \quad K_{\rm sym} = 9\rho^2\left(\frac{\partial^2 E_{\rm sym}}{\partial\rho^2}\right)_{\rho=\rho_0}.$$

Here $L_{\rm sym}$ is the slope parameter defined as the slope of $E_{\rm sym}$ at saturation. The quantity $K_{\rm sym}$ represents the curvature of $E_{\rm sym}$ with respect to density. A large number of investigations have been made to fix the value of $E_{\rm sym}$, $L_{\rm sym}$, and $K_{\rm sym}$ [11,59,63,66–69]. In Fig. 8, we have given the symmetry energy with its first derivative at saturation density with different values of coupling strength starting from $g_\delta = 0.0$–0.6. The variations of $E_{\rm sym}$, $L_{\rm sym}$, and $K_{\rm sym}$ with g_δ are listed in Table I. The variation in symmetry energy takes place from 36.48 to -0.89 MeV, $L_{\rm sym}$ from 100.91 to 28.71 MeV, and $K_{\rm sym}$ from -7.57 to 322.51 MeV at saturation density corresponding to $0.0 \leqslant g_\delta \leqslant 1.0$. The pure G2 set

(0.755, 0.0) is not sufficient to predict this constraint on E_{sym} and L_{sym}. It is suggested to introduce the δ meson as an extra degree of freedom into the model to bring the data within the prediction of experimental and other theoretical constraints. From this investigation, one can see that the permissible values of E_{sym}, L_{sym}, and K_{sym} are not obtained by all the combinations of g_ρ and g_δ. Thus, it is needed to choose a suitable set of g_ρ and g_δ for a proper parametrization both for finite nuclei and infinite nuclear matter. The above tabulated results are also depicted in Fig. 9 to get a graphical representation of E_{sym}, L_{sym}, and K_{sym}. All the three quantities vary substantially with g_δ as shown in the figure. The slope parameter L_{sym} and symmetry energy E_{sym} decreases with g_δ to an exponential increase of K_{sym}.

F. Neutron star

In this section, we study the effect of the δ meson on the mass and radius of a neutron star. Recently, an experimental observation predicted the constraint on the mass of a neutron star and its radius [54]. This observation suggests that the theoretical models should predict the star mass and radius as $M \geqslant (1.97 \pm 0.04)M_\odot$ and $11 < R(\mathrm{km}) < 15$. Keeping this point in mind, we calculate the mass and radius of a neutron star and analyze their variation with g_δ.

In the interior part of a neutron star, the neutron chemical potential exceeds the combined mass of the proton and electron. Therefore, asymmetric matter with an admixture of electrons rather than pure neutron matter, is the more likely composition of matter in neutron star interiors. The concentrations of neutrons, protons, and electrons can be determined from the condition of β equilibrium $n \leftrightarrow p + e + \bar{\nu}$ and from charge neutrality, assuming that neutrinos are not degenerate. Here n, p, e, ν are have the usual meaning as neutron, proton, electron, and neutrino. In the momentum conservation condition $\nu_n = \nu_p + \nu_e$, $n_p = n_e$, where $\nu_n = \mu_n - W + \frac{1}{2}R$ and $\nu_p = \mu_p - W - \frac{1}{2}R$, where $\mu_n = \sqrt{(k_{fn}^2 + M^{*2}{}_n)}$ and $\mu_p = \sqrt{(k_{fp}^2 + M^{*2}_p)}$ are the chemical potentials, and k_{fn} and k_{fp} are the Fermi momentum for the neutron and proton, respectively. Imposing these conditions, in the expressions of $\mathcal{E}$ and $\mathcal{P}$ [Eqs. (20)–(21)], we evaluate $\mathcal{E}$ and $\mathcal{P}$ as a function of density. To calculate the star structure, we use the Tolman-Oppenheimer-Volkoff (TOV) equations for the structure of a relativistic spherical and static star composed of a perfect fluid derived from Einstein's equations [74], where the pressure and energy densities obtained from Eqs. (20) and (21) are the inputs. The TOV equation is given by [74]

$$\frac{d\mathcal{P}}{dr} = -\frac{G}{r}\frac{[\mathcal{E}+\mathcal{P}][M+4\pi r^3\mathcal{P}]}{(r-2GM)}, \qquad (35)$$

$$\frac{dM}{dr} = 4\pi r^2\mathcal{E}, \qquad (36)$$

with G as the gravitational constant and $M(r)$ as the enclosed gravitational mass. We have used $c = 1$. Given the $\mathcal{P}$ and $\mathcal{E}$, these equations can be integrated from the origin as an initial value problem for a given choice of central energy density, (ε_c). The value of $r(=R)$, where the pressure vanishes defines the surface of the star.

The results of mass and radius with various δ-meson coupling strength g_δ is shown in Fig. 10. In the left panel, the neutron star mass with density (gm/cm^3) is given, where we can see the effect of the newly introduced extra degree of freedom δ meson into the system. On the right side of the figure, $M/M_\odot$ is depicted with respect to radius (km), where M is the mass of the star and $M_\odot$ is the solar mass. Here, we used the different set of g_ρ and g_δ coupling constants for calculating the star properties. From this observation, we can say that the δ meson is important not only for the asymmetric system normal density, but also is substantially effective in the high density system. If we compare these results with the previous results [11], i.e., with the effects of the cross coupling of ω-ρ on the mass and radius of a neutron star, the effects are opposite to each other. That means the star masses decreases with Λ_v, whereas it increases with g_δ. Thus a finer tuning in the mass and radius of a neutron star is possible by a suitable adjustment on the g_δ value in the extended parametrization of G2 + Λ_v + g_δ to keep the star properties within the recent experimental observations [54].

IV. SUMMARY AND CONCLUSIONS

In summary, we discussed the effects of cross coupling of ω-ρ mesons in finite nuclei on top of the pure G2 parameter set. The variations of binding energy, rms radii, and energy levels of protons and neutrons are analyzed with increasing values of Λ_v. The change in neutron distribution radius r_n with Λ_v is found to be substantial compared to the less effectiveness of the binding energy and proton distribution radius for the two representative nuclei ^{48}Ca and ^{208}Pb. Thus, to fix the neutron distribution radius depending on the outcome of the PREX experimental [16] result, the inclusion of the Λ_v coupling strength is crucial. This also helps the need of nuclear equation of states as is discussed widely by various authors [10,11]. In the second part of our analysis, for the sensitivity of the δ-meson coupling, we have fixed the binding energies of ^{48}Ca and ^{208}Pb and reshuffled the coupling constants g_ρ and g_δ. With these obtained combinations (g_ρ, g_δ), we evaluated the root mean square radius, binding energy, single particle energy, density, and spin-orbit interaction potential for ^{48}Ca and ^{208}Pb.

We find a substantial contribution comes from the δ-meson coupling, both in finite and infinite nuclear matter, and very different in nature, which may be helpful to fix various experimental constraints. For example, with the help of g_δ, it is possible to modify the binding energy, charge radius, and flipping of the orbits in asymmetric finite nuclei. The nuclear equation of state can be made stiffer with the inclusion of δ-meson coupling. On the other hand, softening of symmetry energy is also possible with the help of this extra degree of freedom. In a compact system, it is possible to fix the limiting values of g_δ and Λ_v by testing the effect of available constraints on symmetry energy and its first derivative with respect to the matter density. This coupling may be useful to fix the mass and radius of a neutron star in light of the recent observation [54]. Thus, we suggest the importance of the inclusion of g_δ coupling in the E-RMF Lagrangian, where, generally, it is ignored in the modern relativistic interaction.

[1] R. J. Furnstahl, B. D. Serot, and H. B. Tang, Nucl. Phys. A **598**, 539 (1996).
[2] R. J. Furnstahl, B. D. Serot, and H. B. Tang, Nucl. Phys. A **615**, 441 (1997).
[3] P. Arumugam, B. K. Sharma, P. K. Sahu, S. K. Patra, Tapas Sil, M. Centelles, and X. Viñas, Phys. Lett. B **601**, 51 (2004).
[4] M. Del Estal, M. Centelles, X. Viñas, and S. K. Patra, Phys. Rev. C **63**, 044321 (2001).
[5] M. Del Estal, M. Centelles, X. Viñas, and S. K. Patra, Phys. Rev. C **63**, 024314 (2001).
[6] Tapas Sil, S. K. Patra, B. K. Sharma, M. Centelles, and X. Viñas, Phys. Rev. C **69**, 044315 (2004).
[7] B. K. Sharma, P. K. Panda, and S. K. Patra, Phys. Rev. C **75**, 035808 (2007).
[8] S. Kubis and M. Kutschera, Phys. Lett. B **399**, 191 (1997).
[9] J. K. Bunta and S. Gmuca, Phys. Rev. C **68**, 054318 (2003).
[10] C. J. Horowitz and J. Piekarewicz, Phys. Rev. Lett. **86**, 5647 (2001); Phys. Rev. C **64**, 062802(R) (2001).
[11] S. K. Singh, M. Bhuyan, P. K. Panda, and S. K. Patra, J. Phys. G: Nucl. Part. Phys. **40**, 085104 (2013).
[12] A. R. Bodmer, Nucl. Phys. A **526**, 703 (1991).
[13] S. Gmuca, Z. Phys. A **342**, 387 (1992); Nucl. Phys. A **547**, 447 (1992).
[14] Y. Sugahara and H. Toki, Nucl. Phys. A **579**, 557 (1994).
[15] B. A. Brown, Phys. Rev. Lett. **85**, 5296 (2000).
[16] S. Abrahamyan *et al.*, Phys. Rev. Lett. **108**, 112502 (2012).
[17] W. H. Long, N. Van Giai, and J. Meng, Phys. Lett. B **640**, 150 (2006).
[18] W. H. Long, H. Sagawa, N. V. Giai, and J. Meng, Phys. Rev. C **76**, 034314 (2007).
[19] W. H. Long, H. Sagawa, J. Meng, and N. Van Giai, Europhys. Lett. **83**, 12001 (2008).
[20] W. H. Long, P. Ring, N. Van Giai, and J. Meng, Phys. Rev. C **81**, 024308 (2010).
[21] H. Liang, P. Zhao, P. Ring, X. Roca-Maza, and J. Meng, Phys. Rev. C **86**, 021302(R) (2012).
[22] N. H. Hugenholtz and W. V. Hove, Physica (Utrecht) **24**, 363 (1958).
[23] Bao-An Li and X. Han, Phys. Lett. B **727**, 276 (2013).
[24] H. Huber, F. Weber, and M. K. Weigel, Nucl. Phys. A **596**, 684 (1996).
[25] H. Huber, F. Weber, and M. K. Weigel, Int. J. Mod. Phys. E **7**, 301 (1998).
[26] J. Leja and S. Gmuca, Acta Phys. Slov. **51**, 201 (2001).
[27] B. Liu, V. Greco, V. Baran, M. Colonna, and M. DiToro, Phys. Rev. C **65**, 045201 (2002).
[28] V. Greco, M. Colonna, M. DiToro, and F. Matera, Phys. Rev. C **67**, 015203 (2003).
[29] S. S. Avancini, L. Brito, D. P. Menezes, and C. Providencia, Phys. Rev. C **70**, 015203 (2004).
[30] T. Gaitanos, M. DiToro, S. Typel, V. Barana, C. Fuchs, V. Greco, and H. H. Wolter, Nucl. Phys. A **732**, 24 (2004).
[31] V. Baran, M. Colonna, V. Greco, and M. DiToro, Phys. Rep. **410**, 335 (2005).
[32] B. Liu, M. DiToro, and V. Greco, Int. J. Mod. Phys. E **17**, 1815 (2008).
[33] H. Pais, A. Santos, and C. Providencia, Phys. Rev. C **80**, 045808 (2009).
[34] A. Rabhi, C. Providencia, and J. DaProvidencia, Phys. Rev. C **80**, 025806 (2009).
[35] G. B. Alaverdyan, Res. Astron. Astrophys. **10**, 1255 (2010).
[36] S. K. Patra and C. R. Praharaj, Phys. Rev. C **44**, 2552 (1991).
[37] Y. K. Gambhir, P. Ring, and A. Thimet, Ann. Phys. (NY) **198**, 132 (1990).
[38] M. Rufa, P.-G. Reinhard, J. A. Maruhn, W. Greiner, and M. R. Strayer, Phys. Rev. C **38**, 390 (1988).
[39] P.-G. Reinhard, M. Rufa, J. Maruhn, W. Greiner, and J. Friedrich, Z. Phys. A **323**, 13 (1986).
[40] M. Sharma, G. A. Lalazissis, and P. Ring, Phys. Lett. B **317**, 9 (1993).
[41] D. Vautherin and D. M. Brink, Phys. Rev. C **5**, 626 (1972).
[42] J. Decharge and D. Gogny, Phys. Rev. C **21**, 1568 (1980).
[43] H. Müller and B. D. Serot, Nucl. Phys. A **606**, 508 (1996).
[44] B. D. Serot and J. D. Walecka, Int. J. Mod. Phys. E **6**, 515 (1997).
[45] P.-G. Reinhard, Rep. Prog. Phys. **52**, 439 (1989).
[46] P. Ring, Prog. Part. Nucl. Phys. **37**, 193 (1996).
[47] D. Vretenar, A. V. Afanasjev, G. A. Lalazissis, and P. Ring, Phys. Rep. **409**, 101 (2005).
[48] J. Meng, H. Toki, S.-G. Zhou, S.-Q. Zhang, W.-H. Long, and L.-S. Geng, Prog. Part. Nucl. Phys. **57**, 470 (2006).
[49] M. Del Estal, M. Centelles, and X. Viñas, Nucl. Phys. A **650**, 443 (1999).
[50] B. D. Serot and J. D. Walecka, Adv. Nucl. Phys. **16**, 1 (1986).
[51] W. Kohn and L. J. Sham, Phys. Rev. **140**, A1133 (1965).
[52] F. Hofmann, C. M. Keil, and H. Lenske, Phys. Rev. C **64**, 034314 (2001).
[53] M. Centelles, S. K. Patra, X. Roca-Maza, B. K. Sharma, P. D. Stevenson, and X. Viñas, J. Phys. G **37**, 075107 (2010).
[54] P. B. Demorest, T. Pennucci, S. M. Ransom, M. S. E. Roberts, and J. W. T. Hessels, Nature **467**, 1081 (2010).
[55] M. Baldo and C. Maieron, Phys. Rev. C **77**, 015801 (2008).
[56] J. Margueron, H. Sagawa, and K. Hagino, Phys. Rev. C **77**, 054309 (2008).
[57] B. Friedman and V. R. Pandharipande, Nucl. Phys. A **361**, 502 (1981).
[58] S. Gandolfi, A. Yu. Illarionov, S. Fantoni, F. Pederiva, and K. E. Schmidt, Phys. Rev. Lett. **101**, 132501 (2008).
[59] M. Dutra, O. Lourenço, J. S. Sá Martins, A. Delfino, J. R. Stone, and P. D. Stevenson, Phys. Rev. C **85**, 035201 (2012).
[60] P. Danielewicz, R. Lacey, and W. G. Lynch, Science **298**, 1592 (2002).
[61] T. Matsui, Nucl. Phys. A **370**, 365 (1981).
[62] X. Roca-Maza, X. Viñas, M. Centelles, P. Ring, and P. Schuck, Phys. Rev. C **84**, 054309 (2011).
[63] M. B. Tsang, J. R. Stone, F. Camera, P. Danielewicz, S. Gandolfi, K. Hebeler, C. J. Horowitz, J. Lee, W. G. Lynch, Z. Kohley, R. Lemmon, P. Möller, T. Murakami, S. Riordan, X. Roca-Maza, F. Sammarruca, A. W. Steiner, I. Vidaña, and S. J. Yennello, Phys. Rev. C **86**, 015803 (2012).
[64] B. K. Agrawal, S. K. Dhiman, and R. Kumar, Phys. Rev. C **73**, 034319 (2006).
[65] B. A. Brown, G. Shen, G. C. Hillhouse, J. Meng, and A. Trzcińska, Phys. Rev. C **76**, 034305 (2007).
[66] C. Xu, B.-A. Li, and L.-W. Chen, Phys. Rev. C **82**, 054607 (2010).

[67] W. G. Newton, M. Gearheart, and B.-A. Li, arXiv:1110.4043.
[68] A. W. Steiner and S. Gandolfi, Phys. Rev. Lett. **108**, 081102 (2012).
[69] F. J. Fattoyev, W. G. Newton, J. Xu, and B.-A. Li, Phys. Rev. C **86**, 025804 (2012).
[70] A. Klimkiewicz *et al.*, Phys. Rev. C **76**, 051603(R) (2007).
[71] A. Carbone, G. Colò, A. Bracco, L.-G. Cao, P. F. Bortignon, F. Camera, and O. Wieland, Phys. Rev. C **81**, 041301(R) (2010).
[72] P. Danelewicz and J. Lee, arXiv:1111.0326v1.
[73] P. Moller, W. D. Myers, H. Sagawa, and S. Yoshida, Phys. Rev. Lett. **108**, 052501 (2012).
[74] J. R. Oppenheimer and G. M. Volkoff, Phys. Rev. **55**, 374 (1939); R. C. Tolman, *ibid.* **55**, 364 (1939).